



Optimization of Intracranial Hemorrhage Using CT Scan Images and Feature Extraction

K. Somasundaram¹, R. Sathish Kumar¹, S. Sanjayprabu¹, R. Karthikamani², S. Sivasankar^{3*}

¹Sri Ramakrishna Mission Vidyalaya College of Arts and Science, Coimbatore, Tamil Nadu, India.

²Sri Ramakrishna Engineering College, Coimbatore, Tamil Nadu, India

³Department of Mathematics, RV Institute of Technology and Management, Bengaluru-560076, India.

*Corresponding author's: S. Sivasankar

Article History	Abstract
Received: 06 June 2023 Revised: 05 Sept 2023 Accepted: 12 Nov 2023	<i>Intracranial bleeding is among the most severe forms of brain stroke. The neurologic effects and artery rupture cause bleeding in the brain and the tissue around it. Haemorrhage is classified based on where the bleeding occurs on the brain. This paper depicts the application of multiple machine-learning approaches to separate CT scan images into normal and pathological categories. Separate analysis is conducted on the functionality of the features extracted from the various texturing approaches, such as the Grey Level Co-occurrence Matrix (GLCM) and Grey Level Run-Length Matrix (GLRLM). Particle Swarm Optimisation (PSO) and K-Nearest Neighbours are used to choose relevant characteristics that increase the classification accuracy for feature extraction. The findings demonstrate that these texture features have excellent discrimination accuracy.</i>
CC License CC-BY-NC-SA 4.0	Keywords: CT, GLCM, GLRLM, PSO, KNN, SVM

1. Introduction

In the medical treatment, a precise diagnosis is essential to hastening the patient's recuperation. Intracranial hemorrhage (ICH), a broad term for the disorder, describes it. Subarachnoid hemorrhage and intracerebral hemorrhage are the two hemorrhages [1]. Bleeding within the real brain tissue is known as an intracerebral hemorrhage. Subarachnoid hemorrhage, on the other hand, results from bleeding near the brain. Examining the patient's physical and medical history is the main strategy for diagnosing ICH. Because 50% of patients pass away within 24 hours, an immediate and precise diagnosis is crucial. After 30 days, the mortality rate rises to 60%, and within a month of entering the critical zone, mortality rates for patients range from 45% to 60%. A stroke is a serious brain condition that requires prompt medical attention. There are significant difficulties to overcome correct ICH diagnosis, time-consuming decision-making process. The insufficient experience that occasionally affects new radiologists may result from their inexperience with making decisions. The physical evaluation of a patient and CT image analysis are some of the traditional approaches. Treatment will be provided by skilled radiologist. It is necessary to provide an automated diagnostic tool to help radiologists to make decisions quickly, so that they can start treating patients more quickly. First hand examination is carried out by proper diagnosis by a medical professional who uses non-contrast computed tomography (CT) analysis to conduct the first-hand evaluation. CT image analysis can pinpoint and locate the site of internal bleeding in the brain [2].

To expedite clinical workflow and shorten diagnosis times, recent scientific inquiries have primarily focused on categorizing, identifying, and raising suspicion regarding cerebral hemorrhages. The categorization approach specifically helps the doctors' become experts in their own accurate picture analysis and differentiation of hemorrhage and normal images -occurrence matrix [2].

Different adaptations and algorithms for pre-trained neural networks are utilized in image analysis, feature extraction, and classification. Specifically, CT scan intracranial images sourced from Kaggle are compared with data from medical databases [3] to discern variations and discrepancies. The Gray Level Co-occurrence Matrix (GLCM) and Gray Level Run Length Matrix (GLRLM) are introduced and [4] are used to extract the features. The proposed feature extraction method from the transformed-based characteristics and GLCM-based characteristics includes the composite feature. An image texture

can be recognized with the help of feature extraction using a GLCM-based method. It is a crucial concept for categorizing images according to their texture. The detection and separation of high-frequency and low-frequency coefficients in input images is also facilitated by transformed-based approaches. As a result, it is simple to produce visualizations from the energy coefficients that contain important information. These two methods are combined in order to create new hybrid features that accurately categorize both normal and abnormal pictures while also accelerating the classification process.

The input data are then classified using K-Nearest Neighbour Classifier and Particle Swarm Optimization (PSO). In order to obtain the most accurate and effective occurrence matrix, this research proposes a useful feature extraction approach and classifier. Here CT scan images are used to diagnose the abnormality of intracranial Hemorrhage with appropriate statistical characteristics and categorization.

This work is organized in a following manner. Intracranial bleeding CT image databases are introduced in Section (1), and data collecting and pre-processing for CT images are covered. In section (2), GLCM feature extraction, GLRLM Feature Extraction and its characteristics in the CT scan are represented. Feature extraction of GLCM and GLRLM Texture data is explained in section (3). Section (4) provides illustrations for the two classifiers. Sections (5) provide the result analysis and remarks. Finally, Section (6) concludes the paper.

2. Materials And Methods

Kaggle is used to gather the standard CT imaging data set for intracranial hemorrhage for brain stroke. A total of 200 CT images, comprising both normal and hemorrhage brain imaging, are included in the data set. The CT scan data is originally in RGB format, and noise has been effectively removed to ensure image accuracy in this phase of the project. During this stage, modifications to the images are made based on MATLAB guidelines for grayscale conversion and noise reduction. Converting the input CT images from RGB to grayscale is a critical step in the pre-processing, as it enhances specific image attributes necessary for subsequent processing and improves the overall image data quality. The steps in pre-processing a CT picture are as follows: Images from an RGB CT scan are converted to grayscale.

Methods

The CT scan image dataset for intracranial hemorrhage is used for feature extraction, and the recovered feature vectors are then used as input for machine learning classifiers.

Figure 1: provides an overview of the entire process, which involves pre-processing the Hemorrhage CT images using suitable filters, followed by the extraction of GLCM features. These features are subsequently fed into two classification models, and the effectiveness of the classifiers being assessed by nine predefined factors.

Figure 2: Describe how the PSNR, SNR, and MSE values are utilized to determine the filtering approach.

Table.1: Wiener Filtered Images (IM)

	IM 0	IM 1	IM 2	IM 3	IM 4	IM 5
PSNR	30.4726	28.3618	28.7921	28.6581	32.025	30.4726
SNR	62	67	55	59	48	62
MSE	58.3207	94.8204	85.8756	88.5663	40.7926	58.3207

Table. 2: Median Filtered Image

	IM 0	IM 1	IM 2	IM 3	IM 4	IM 5
PSNR	34.8071	30.5526	32.7056	33.0713	37.7418	38.1468
SNR	136	188	75	70	52	59
MSE	21.4967	57.2566	34.8756	32.059	10.9369	9.9633

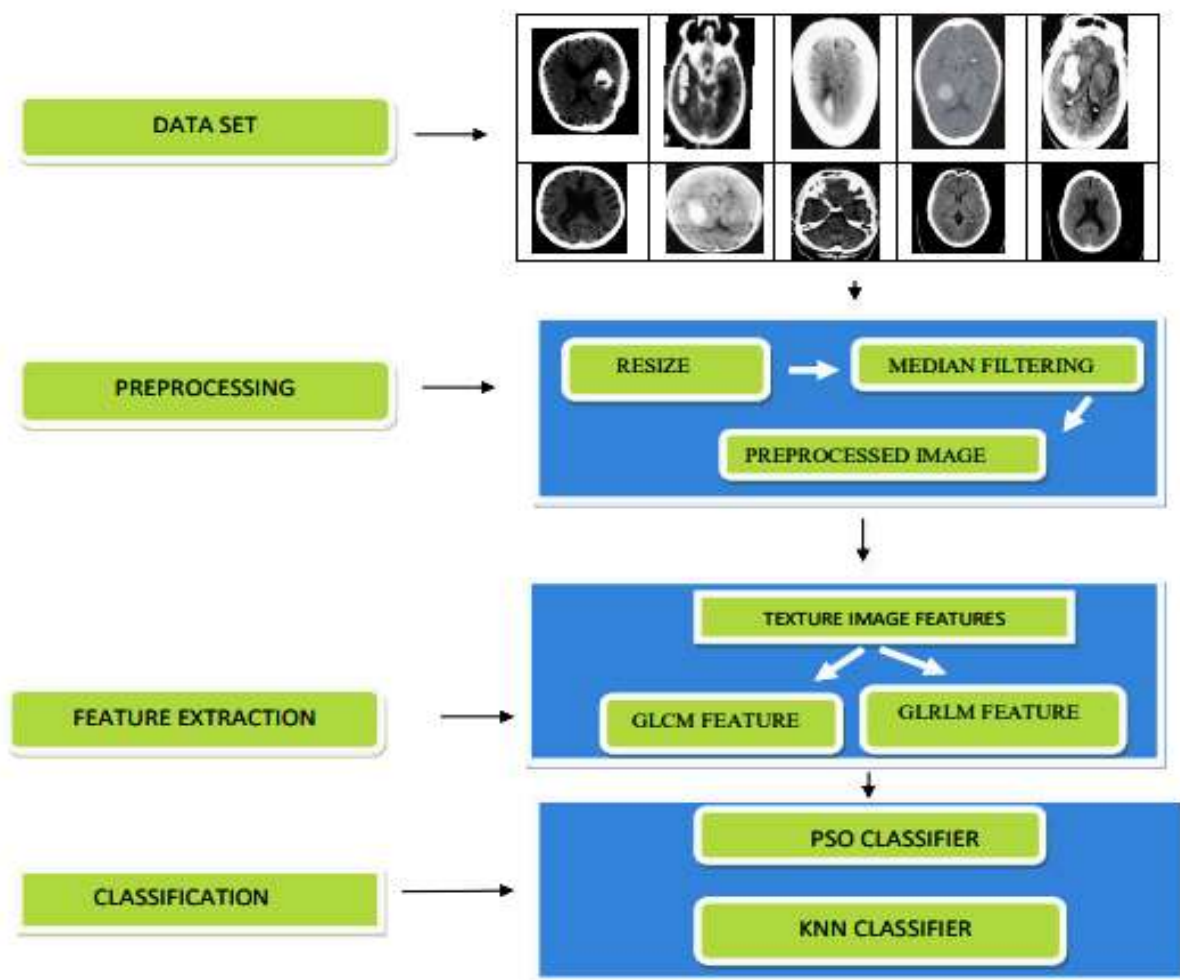


Figure. 1 System Overview

Feature Extraction

Gray Level Co-occurrence Matrixes

The method of texture-based feature extraction known as the Grey-Level Co-occurrence Matrix (GLCM) holds a significant position. It defines the relationship between pixels in terms of texture by conducting operations based on the second-order statistics of the image. Typically, this technique [5] involves analyzing pairs of adjacent pixels. The GLCM figures out the frequency of pairs of pixel luminance values, which basically tells you how often pixel pairs happen [6]. In the picture, these GLCM features are shown as a matrix, with the same number of rows and columns as gray levels in the picture. The entries within this matrix are determined by the repetitions of occurrences of the two supplied pixels, which can vary based on their respective surroundings. The matrices entries have probability values derived from second-order statistics, shedding light on the relationships among pixels within the region.

To depict pixel relationships within a region and build the Grey-Level Co-occurrence Matrix, the GLCM is utilized. It relies on inferring second-order mutual limited probability density functions $P(i, j | d, \theta)$ for a variety of directions, usually denoted by $\theta = 0$. A prominent feature extraction method rooted in image texture analysis is the Grey-Level Co-occurrence Matrices (GLCM) [9], which leverages the concept of pixel intensity distribution.

In this study, a range of essential GLCM features are utilized, encompassing perfect correlation, disparity, correlation, cluster eminence, greatest probability, sum of squares (variance), total mean, total variation, entropy total, differentiation variation, differentiation entropy, information correlation estimate, inverse differentiation normal form, and normal form inverse differentiation moment. By leveraging these properties, a comprehensive GLCM feature matrix is constructed, providing an effective description of an image with a reduced set of parameters.

Table 3: GLCM Texture values for Abnormal CT Scan images (IM)

Sl.No	Attributes	IM 1	IM 2	IM 3	IM 4
1	Autocorrelation	18.5323368	22.1693122	13.6320706	17.0251015
2	Contrast	0.17694477	0.40168519	0.2424738	0.25855037
3	Correlation(M)	0.98643225	0.96625692	0.97874905	0.98073436
4	Correlation(P)	0.98643225	0.96625692	0.97874905	0.98073436
5	Cluster Prominence	1495.82415	1091.68152	1664.76916	1681.77742
6	Cluster Shade	112.960875	40.3130259	135.831972	130.352682
7	Dissimilarity	0.12413243	0.18814654	0.16211417	0.174227
8	Energy	0.17208425	0.13814982	0.23576159	0.19089985
9	Entropy	2.14026395	2.37903267	2.03295724	2.18769488
10	Homogeneity(M)	0.9448439	0.92406853	0.92895159	0.92344219
11	Homogeneity	0.94300352	0.92184371	0.92651504	0.92081987
12	Greatest probability	0.26151981	0.22706862	0.43257299	0.35645697
13	Sum of squares	18.5211864	22.2471433	13.6648968	17.0536285
14	total average	6.95718995	8.10386236	5.67391134	6.46351344
15	total variance	50.3392578	58.2330992	37.0195469	46.3892504
16	total entropy	2.01397902	2.2024451	1.87365689	2.01298663
17	Differentiation variance	0.17694477	0.40168519	0.2424738	0.25855037
18	Differentiation Entropy	0.38685157	0.48949156	0.46423571	0.48823304
19	Information estimates of correlation1	-0.7724447	-0.7245617	-0.7128313	0.48823304
20	Information estimates of correlation2	0.96553566	0.96590675	0.94584807	0.95331103
21	Inverse differentiation normalized	0.9867439	0.98089785	0.98278817	0.98148277
22	Inverse differentiation moment normalized	0.99741476	0.99501098	0.99650046	0.99626391

Table 4: GLCM Texture values for Normal CT Scan images

Sl.No	Attributes	IM 1	IM 2	IM 3	IM 4
1	Perfect correlation	13.8621376	15.3177801	20.63328102	19.46708307
2	Contrast	0.2785928	0.27730584	0.210249451	0.350579565
3	Correlation(M)	0.96530644	0.96713734	0.969577111	0.960041277
4	Correlation(P)	0.96530644	0.96713734	0.969577111	0.960041277
5	Cluster Prominence	951.796953	903.2443	539.1090389	745.1735941
6	Cluster Shade	71.9507694	59.1183317	10.22775937	17.14279345
7	Dissimilarity	0.18367036	0.17841289	0.174000749	0.177939069
8	Energy	0.21530341	0.18780111	0.180941762	0.166098624
9	Entropy	2.07357653	2.11655363	2.289152968	2.252983235
10	Homogeneity(M)	0.92163943	0.9245218	0.918808556	0.928266885
11	Homogeneity	0.91751743	0.92046118	0.916624496	0.925523045
12	Greatest probability	0.36172789	0.25666002	0.36319449	0.277337532
13	Sum of squares	13.9037782	15.3497661	20.62601809	19.52231588
14	total average	13.9037782	6.70432638	8.314667579	7.811629988
15	total variance	6.32024947	39.3469743	52.0578239	50.05140887
16	total entropy	1.88861212	1.9350132	2.114019729	2.07979215
17	Differentiation variance	0.2785928	0.27730584	0.210249451	0.350579565
18	Differentiation Entropy	0.50693619	0.49631769	0.489208057	0.478346503
19	Information estimates of correlation1	-0.6955691	-0.7065472	0.708302796	-0.72047742
20	Information estimates of correlation2	0.94357628	0.94918371	0.958548689	0.959598434
21	Inverse differentiation normalized	0.98058716	0.98120374	0.98106371	0.981800887
22	Inverse differentiation moment normalized	0.99591624	0.99595773	0.996821137	0.99534785

Gray Level Run Length Matrix

The Grey Level Run Length Matrix (GLRLM) is a texture representation model that leverages higher-order statistics to capture the spatial plane features of each pixel [11]. Following this process, a 2D feature matrix is generated, with each element representing the overall count of grey level occurrences

in a specific direction [5]. Let's denote P (i, j) as the image matrix utilized in this study to establish the GLRLM properties. The property matrix is derived using the following formulas:

Table 5. Formulae of GLRLM Feature Extraction

S.No	FEATURES	FORMULAE
1	RUN LENGTH NON-UNIFORMITY - RLN	$\sum_{i=1}^R \left[\sum_{j=1}^G P(i,j) \right]^2$
2	GREY LEVEL NON-UNIFORMITY - GLN	$\sum_{i=1}^G \left[\sum_{j=1}^R P(i,j) \right]^2$
3	RUN PERCENTAGE - RP	$RP = \frac{1}{n} S$
4	LONG RUN EMPHASIS (LRE) - LRE	$\sum_{i=1}^G \sum_{j=1}^R j^2 P(i,j)$
5	SHORT RUN EMPHASIS - SRE	$\sum_{i=1}^G \sum_{j=1}^R \frac{P(i,j)}{j^2}$
6	HIGH GREY LEVEL RUN EMPHASIS - HGRE	$\sum_{i=1}^G \sum_{j=1}^R i^2 P(i,j)$
7	LOW GREY LEVEL RUN EMPHASIS - LGRE	$\sum_{i=1}^G \sum_{j=1}^R \frac{P(i,j)}{j^2}$

Table 6: GLRLM Texture values of Abnormal CT Scan Images (IM)

Sl.No	Features	IM 1	IM 2	IM 3	IM 4
1	SHORT RUN EMPHASIS	0.4483	0.4608	0.5195	0.5186
2	LONG RUN EMPHASIS	92.7829	72.5569	149.4451	99.9895
3	GREY LEVEL NON - UNIFORMITY	5636.362	6076.2778	5927.1929	5848.9806
4	RUN PERCENTAGE	0.9017	1.0195	0.9192	1.0121
5	RUN LENGTH NON-UNIFORMITY	12092.9864	14680.4789	15763.6211	17307.039
6	LOW GREY LEVEL RUN EMPHASIS	60.3	76.0442	51.7183	58.4596
7	HIGH GREY LEVEL RUN EMPHASIS	5636.362	6076.2778	5927.1929	5848.9806

Table 7: GLRLM Texture values of Normal CT Scan Images (IM)

Sl.No	Features	IM 1	IM 2	IM 3	IM 4
1	SHORT RUN EMPHASIS	0.4683	0.4775	0.4583	0.3821
2	LONG RUN EMPHASIS	108.3494	107.4961	95.0811	100.6734
3	GREY LEVEL NON - UNIFORMITY	5467.0574	4769.2782	4016.4029	5474.2661
4	RUN PERCENTAGE	0.8057	0.7799	0.7702	0.7999
5	RUN LENGTH NON-UNIFORMITY	11089.7271	11083.948	10270.3965	8333.3625
6	LOW GREY LEVEL RUN EMPHASIS	68.6872	71.5618	101.2308	83.5017
7	HIGH GREY LEVEL RUN EMPHASIS	5467.0574	4769.2782	4016.4029	5474.2661

Classification

Particle Swarm Optimization (PSO)

Particle Swarm Optimization (PSO) is an optimization technique inspired by the collective behavior observed in flocks of birds, operating on a population-based approach [6, 15]. The PSO algorithm begins with a set of random particles and iteratively searches for the best solution by updating

generations. Each particle traverses through the search space, adjusting its position based on its distance from its own optimal position and the optimal position within the swarm. A fitness function, which gauges proximity to the ideal solution, is used to evaluate each particle's performance.

Each particle, denoted as 'I', navigates an n-dimensional search space R^n and retains the following information:

y_i , the present position of i^{th} particle (y –vector),

q_i , the personal best position of i^{th} particle (q –vector)

V_i , the current velocity of i^{th} particle (V –vector)

For a particle 'i', its personal best position is defined as the best location the particle has encountered up to that point. If 'g' represents the fitness function, the update for the personal best of particle 'i' at time step 't' is expressed as follows:

$$q_i(t+1) = q_i(t) \quad \text{if} \quad \begin{cases} g(y_i(t+1)) \geq g(q_i(t)) \\ y_i(t+1) \quad \text{if} \quad g(y_i(t+1)) < g(q_i(t)) \end{cases} \quad (1)$$

If gbest denotes the global best particle's position, then

$$g_{best} \in \left\{ q_1(t), q_2(t), q_3(t), q_4(t) \dots q_m(t) \right\} \\ = \min \left\{ g(q_1(t), q_2(t), q_3(t), q_4(t) \dots q_m(t)) \right\} \quad (2)$$

The updates to velocity are computed based on the position and velocity vectors. Therefore, with the help of equation (3), the velocity of particle 'i' undergoes an update, and utilizing equation (4), the position of particle 'i' is then updated.

$$V_i(t+1) = wV_i(t) + c_1r_1(q_i(t) - y_i(t)) + c_2r_2(g_{best} - y_i(t)) \quad (3)$$

$$y_i(t+1) = y_i(t) + v_i(t+1) \quad (4)$$

In the given equation, 'w' stands for the inertia weight, 'c1' and 'c2' are acceleration constants, 'r1' and 'r2' are random numbers within the interval [0,1], and V_{max} is the maximum velocity. It's essential to emphasize that 'r1' and 'r2' must fall within the [0,1] range, while 'Vmax' needs to be within the designated interval [-Vmin, Vmax), where 'Vmin' represents the minimum velocity.

K-Nearest Neighbours (KNN)

The K-Nearest Neighbors (KNN) algorithm is considered a nonparametric technique in the field of machine learning. When it comes to learning and prediction analysis, the approach is tailored to the specific problem or dataset in question. In the classification model of K-Nearest Neighbors, predictions are made solely based on the values of neighboring data points, without making any underlying assumptions about the dataset. In K-Nearest Neighbors, the 'K' signifies the count of nearest neighbor data points. Using this 'K' value, the KNN algorithm determines the classification of the given dataset. The K-Nearest Neighbors model classifies the training dataset directly. Essentially, when predicting a new instance, the algorithm identifies the 'K' closest neighbor instances within the training set by employing the Euclidean distance formula. Subsequently, it classifies the new instance based on the class that is most prevalent among those 'K' neighbor instances. The determination of similarity between instances is done using the Euclidean distance, calculated as the square root of the sum of squared differences between the new instance (x_i) and the corresponding coordinates of the existing instance (y_j).

$$Euclidean_{i,j} = \sqrt{\sum_{k=1}^n (x_{ik} - y_{jk})^2} \quad (5)$$

3. Results and Discussion

The database employed for generating the input images comprises a total of 200 CT images per head. These images are divided into two distinct categories: Abnormal and Normal Images. In this experiment, both PSO and KNN classifiers receive input from two distinct types of feature extraction

values. Following this, the performance of these feature approaches is evaluated using shared parameters.

Table 8. Confusion Matrix for PSO with GLCM

		Actual Values	
		Positive (1)	Negative (0)
Predicted Values	Positive (1)	95	5
	Negative (0)	3	97

Table 9. Confusion Matrix for KNN with GLCM

		Actual Values	
		Positive (1)	Negative (0)
Predicted Values	Positive (1)	97	3
	Negative (0)	2	98

Table.10 Confusion Matrix for PSO with GLRLM

		Actual Values	
		Positive (1)	Negative (0)
Predicted Values	Positive (1)	90	10
	Negative (0)	15	85

Table 11. Confusion Matrix for KNN with GLRLM

		Actual Values	
		Positive (1)	Negative (0)
Predicted Values	Positive (1)	88	12
	Negative (0)	20	80

Based on the aforementioned data, standard parameters such as sensitivity, specificity, and accuracy are computed for all the feature extraction techniques. These metrics are organized and presented in Table 5. The following formulas are employed to determine the standard parameters.

$$Sensitivity = \frac{TP}{TP + FN} * 100\% \dots\dots\dots (6)$$

$$Specificity = \frac{TN}{TN + FP} * 100\% \dots\dots\dots (7)$$

The accuracy of a test lies in its capability to accurately differentiate between patients and healthy cases. To assess this accuracy, it's vital to calculate the proportion of true positive and true negative results among all the cases analyzed. This can be represented mathematically as:

$$Accuracy = \frac{TP + TN}{TP + TN + FP + FN} * 100 \dots\dots\dots (8)$$

True Positive (TP) - This happens when patients who are truly ill are correctly identified as such. False Positives (FP) occur when healthy individuals are incorrectly classified as ill. True Negatives (TN) are instances where healthy individuals are correctly identified as not ill. False Negatives (FN) occur when sick individuals are incorrectly classified as healthy [15].

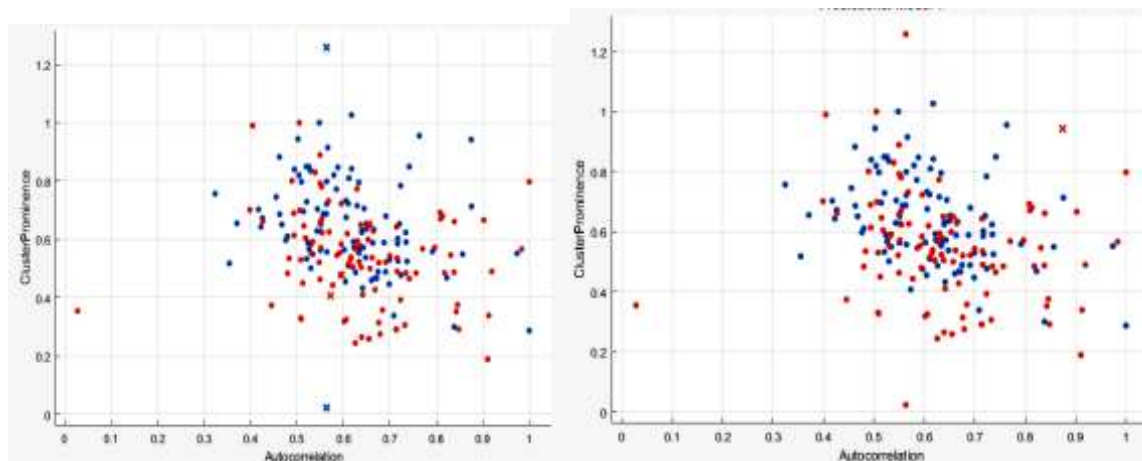


Figure 2. Scatter Plot of GLCM Features with PSO and KNN

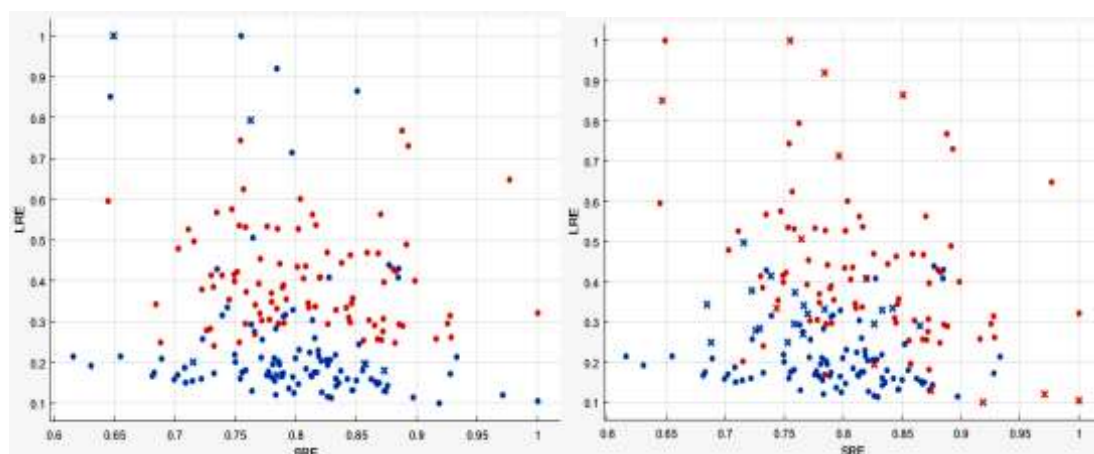


Figure 3. Scatter Plot of GLRLM Features with PSO and KNN

Table 12. Performance analysis of Classifiers

Parameters (%)	GLCM		GLRLM	
	PSO	KNN	PSO	KNN
Sensitivity	96.93878	97.9798	85.71429	81.48148
Specificity	95.09804	97.0297	89.47368	86.95652
Accuracy	96	97.5	87.5	84
Error rate	4	2.5	12.5	16
Precision	95	97	90	88
F1 Score	95.9596	97.48744	87.80488	84.61538
Jacard Metric	92.23301	95.09804	78.26087	73.33333
Balanced Classifier Rate	96.01841	97.50475	87.59398	84.219
MCC	0.920184	0.950048	0.750939	0.682187

Table (12) displays the evaluation metrics. Specifically, the KNN classifier is presented using two features. Notably, the GLCM features achieve an impressive accuracy of 97.5%. In contrast, when utilizing GLRLM with KNN, the classification rate drops to 84%, indicating a relatively lower performance.

4. Conclusion

The analysis of GLCM and GLRLM feature extraction performance is conducted using MATLAB software. Filtering is applied based on Mean Squared Error (MSE), Peak Signal-to-Noise Ratio (PSNR), and Signal-to-Noise Ratio (SNR) values to enhance image quality. A median filter is employed to effectively remove image noise. The GLCM and GLRLM feature extraction methods calculate average values, and a normalized scatter plot is generated to illustrate the identification of normal and abnormal images. Two classifiers are utilized to detect abnormalities related to Head Hemorrhage. Notably, the KNN classifier with GLCM achieves a higher average accuracy of 97.5% compared to other classifiers. In summary, this approach facilitates the straightforward identification of Head Hemorrhage within the dataset.

References:

1. Marcolini.E, Stretz.C , DeWitt. K.M . Intracranial Haemorrhage and Intracranial Hypertension. *Emerg.Med.Clin. N. Am.* 2019, 37,529–544.
2. Castro.j, Chabert.S , Saavedra.C , Salas. R. Convolutional neural networks for detection of intracranial haemorrhage in CT images. In *Proceedings of the 5th Congress on Robotics and Neuroscience*, Valparaíso, Chile, 27–29 February 2020; Volume 2564.
3. Albregtsen.F, Nielsen.B & Danielsen.H.E.(2000). Adaptive gray level run length features from class distance matrices. In *Pattern Recognition, 2000. Proceedings. 15th International Conference on* (Vol. 3, pp. 738-741). IEEE.
4. Mohanaiah.P , Sathyanarayana.P , & GuruKumar. L, (2013). Image texture feature extraction using GLCM approach. *International Journal of Scientific and Research Publications*,3 (5), 1.
5. A.Aafreen Nawresh. S.Sasikala, An Approach for efficient classification of CT scan Brain Hemorrhage types using GLCM features with multilayer perceptron ICDSMLA 201 (pp.400-412),Springer Nature.
6. Shirvaikar.N. Huang, and X. N.Dong. “The Measurement of Bone Quality Using Gray Level Co-Occurrence Matrix Textural Features,” *J. Med. Imaging Heal. Informatics*, vol. 6, no. 6, pp. 1357–1362, 2016.
7. Latchoumi.T.P, Parthiban.L, Abnormality detection using weighed particle swarm optimization and smooth support vector machine. (2017).
8. Chilamkurthy.S , Ghosh.R , Tanamala.S et al (2018) Development and validation of deep learning algorithms for detection of critical findings in head CT scans.arXiv preprint arXiv:1803.05854.
9. Karki.M , Cho,J , Lee,E , Hahm,M.H , Yoon,S.Y, Kim,M . Ahn,J.Y , Son,J, Park.S.H.,Kim.K.H.and Park.S.2020. CT window trainable neural network for improving intracranial hemorrhage detection by combining multiple settings. *Artificial Intelligence in Medicine*, p.101850.
10. Latchoumi.T.P, Balamurugan.K, Dinesh.K, Ezhilarasi.T.P Particle Swarm Optimization approach for waterjet cavitation peening. *Measurement*, (2019) 141, 184-189.
11. R. Karthikamani, Harikumar Rajaguru, Detection of Liver Cirrhosis in Ultrasonic Images from GLCM Features and Classifiers, S. Vlad and N. M. Roman(Eds.): *MEDITECH 2020, IFMBE,Proceedings.88*,Springer,pp.161–172,2022.https://doi.org/10.1007/978-3-030-93564-1_1
12. Mohanty.A.K, Beberta.S, and Lenka.S.K.(2011). Classifying benign and malignant mass using GLCM and GLRLM based texture features from mammogram. *International Journal of Engineering research and Applications*, 1(3), 687-693.
13. Pang. J., Zhang.S., and Zhang.S.(2016, May). A median filter based on the proportion of the imagevariance. In *Information Technology,Networking, Electronic and Automation Control Conference*, IEEE (pp. 123-127). IEEE.
14. Sivakumar Sanjayprabu , Sathish Kumar Rangasamy,R , Somasundaram Kuppusamy and Ramamoorthy Karthikamani (2022). Mathematical Model for Anisotropic diffusion Filter and GLRLM Feature Extraction to Detect Covid-19 from Chest X-Ray Images. 1-5. <https://doi.org/10.1109/STCR55312.2022.10009430>.